Progress In Electromagnetics Research C, Vol. 135, 227–240, 2023

EBG Integrated Metasurface Antenna for SAR Reduction

Kaliappan Kavitha*, Selva Vijay Gokul, Sivakumar Yazhini, J. M. Kanaka Durga, and Raja Keerthana

Abstract—This research article presents an innovative design of a textile-based microstrip patch antenna with a metasurface for medical applications. The antenna is designed to operate at a frequency of 2.4 GHz, which is the frequency of the Industrial, Scientific, and Medical (ISM) band, to minimize the Specific Absorption Rate (SAR) in the human body. The design includes an Electromagnetic Band Gap (EBG) that is placed above a metasurface, which is made up of a periodic array of I-shaped structures. A foam layer is placed between the EBG and the antenna to improve performance. The use of textile-based materials in the antenna allows for flexibility and comfort when it is mounted on the human body. The integration of the metasurface in the antenna design allows for a more efficient transfer of energy from the antenna to the surrounding tissue, resulting in a reduction in the amount of energy absorbed by the body. The simulation of the antenna design is carried out using Computer Simulation Technology (CST), which provides accurate results for the performance of the antenna. After the implementation of the EBG array, the gain of the antenna is improved, resulting in better performance. The proposed antenna design achieved a SAR value of 0.077 W/kg over 1 gram of thigh tissue, which is well below the safety limit set by the International Commission on Non-Ionizing Radiation Protection (ICNIRP). This implies that the integrated design of the antenna can be safely used in medical applications.

1. INTRODUCTION

In recent times, textile-based patch antennas have become increasingly popular due to their light weight, flexibility, and conformal nature [1]. They find applications in wearable technology, healthcare, and communication systems. However, their low gain, efficiency, and narrow bandwidth limit their use in practical applications [2]. To overcome these limitations, researchers have explored the use of metasurfaces, which are artificial structures composed of subwavelength units that manipulate electromagnetic waves' behavior [3, 4]. An electromagnetic bandgap structure (EBG) has been designed underneath the antenna to upgrade the antenna performance [5, 6]. This study will discuss the design and simulation of a textile-based patch antenna with a metasurface (MS) and EBG structure.

Metamaterials are artificial materials where properties are not found in nature [7]. They are widely studied in the field of antenna design as they possess the characteristics of manipulating electromagnetic waves in unconventional ways. In recent days, metasurfaces have gained attention for their ability to manipulate the reflection and transmission of electromagnetic waves with high efficiency and low losses.

Jiang et al. (2014) proposed a metasurface-enabled conformal antenna for WBAN devices [8]. Here, the antenna showed a reflector type of artificial magnetic conductor (AMC), a gain of 6.2 dBi, and efficiency not available. The values of SAR were also analyzed and found to be 0.66 W/kg over 1 g of tissue. Wang et al. (2018), described a flexible antenna using metamaterial [9]. The antenna showed a gain of 5.2 dBi. The efficiency of the designed antenna was reported to be around 61.3%. The SAR values were found to be 2.48 (W/kg) below the safety limits set by the ICNIRP.

Received 13 May 2023, Accepted 10 July 2023, Scheduled 7 August 2023

* Corresponding author: Kaliappan Kavitha (kavi@vcet.ac.in).

The authors are with the Centre for RF Circuits and Antenna Design, Department of Electronics and Communication Engineering, Velammal College of Engineering and Technology (Autonomous), Madurai, India.

Zhang et al.'s publication [10] (2020) presented a metasurface-based compact wearable antenna, which exhibited a gain of 2.99 dBi and a 300 MHz bandwidth. This design is particularly well-suited for monitoring vital-sign data in health monitoring systems within the ISM band, and it could be used in WBAN applications such as smart bracelets or watches. Purohit and Raval [11] analyzed a body worn textile antenna that operated at 2.45 GHz and used jeans as its substrate. The use of textile material with a low dielectric constant (ranging from 1 to 2) helped to reduce surface wave losses and improved antenna bandwidth. The designed antenna exhibited a gain of 7.2 dBi and a return loss of −32.57 dB. Janapala et al. [12] presented a flexible antenna using polydimethylsiloxane with a leaf-like structure covering the WLAN ISM band of 2.4 GHz, integrated with a metasurface unit cell. The study reported a SAR of 2.53 W/kg for a tissue volume of 1 g.

Sheeba and Jayanthy [13] examined the use of several ISM band feeding strategies with a microstrip antenna composed of lightweight substrates. The study involved comparing several parameters such as return loss, dielectric constant, gain, and directivity. The research revealed that the impedance matching for textile antennas is affected significantly by E-plane bending. Youssef et al. [14] developed a fully fabricated I-shaped patch antenna that was integrated with a textile-based AMC employed in low SAR wearable applications. By integrating an AMC array, the gain of the antenna was improved by 75%, and a significant reduction in SAR was achieved. Iqbal and Kha [15] utilized methods such as Kramers-Krong and Nicolson Rose Weir (NRW) to analyze metasurfaces and extract numerical parameters for their application in antennas, specifically through unit cell design.

Agus et al. [17] illustrated a meta-wearable textile Multiple-Input and Multiple-Output (MIMO) antenna using viscose-wool felt. The antenna design incorporated Reflecting and Electromagnetic Band Gap (RIS and EBG) surfaces to improve gain and bandwidth. The SAR values for the antenna were evaluated, and the results showed that they were within the permissible limits established by the ICNIRP guidelines. To mitigate undesired surface waves, Althuwayb et al. created an EBG decoupling structure that isolated the radiating elements [18]. The modifications made to the antenna design significantly reduced the unwanted surface waves. The antenna also showed excellent wideband performance, with a radiation efficiency of 80% and a gain of 9.50 dBi.

Kumar et al. [19] designed an antenna using a mushroom-type EBG to limit the surface waves of the antenna by utilizing the band-stop frequency characteristic of EBG structures. Additionally, the implementation of mushroom-type EBG structures results in a notable 5.9% increase in the antenna's bandwidth. In the study by Gnanagurunathan and Udofia [20], an EBG-enclosed patch antenna was designed. Here the positioning of EBG cells contributed towards beamwidth increment, back lobe reduction, and bidirectional radiation properties. The study also found that a back lobe reduction of almost 100% can be achieved by offsetting the distance by 0.8 mm. Finite-Difference Time-Domain (FDTD) method was utilized to study how a wave source interacts with the human head. The investigation was carried out, and the averaged SAR computed was 0.0143 W/kg and 0.0153 W/kg for sagittal and coronal cases, respectively. In the sagittal incidence case, the tissue-averaged SARs were found to be significantly higher than in the coronal case. The study by Akram and Jasmy [23] revealed that the tissue-averaged SARs differed considerably while the head-averaged SARs were similar for both cases at a frequency of 900 MHz.

Gao et al. in 2018 proposed a wearable circular ring antenna for wireless communication applications [24]. This antenna showed a gain of 3.5 dBi and a reflector type of EBG. The efficiency of the antenna was reported to be around 55%. The SAR values of the antenna were also analyzed and found to be 0.55 W/kg below the safety limits set by the ICNIRP. Balaji Vignesh and Kavitha [25] explored fractal antennas' utility in meeting the demand for small, wideband, and multiband antennas across diverse applications such as cellular phones, airplanes, spacecraft, and missiles. While these antennas offer compact size and frequency versatility, they face limitations such as low gain and bandwidth. Fractal geometry can mitigate these limitations by cutting slots, reducing the antenna's metallic material, and producing multiband or wideband capabilities. Moreover, it improves bandwidth, making it suitable for ISM band and WLAN applications.

In contrast, our study delves into the design and analysis of metasurface reflectors with distinct unit cell configurations to reduce SAR in wireless communication applications. Our proposed antennas with 1×1, 2×2, and 3×3 metasurface reflectors succeed in lowering SAR in skin, muscle, and fat tissues of different thicknesses while maintaining high antenna performance in directivity, efficiency,

gain, and return loss. The results reveal the potential of metasurfaces for SAR reduction in wireless communication systems.

The remainder of this paper is as follows. The antenna study analysis and design methodologies are detailed in the first section of this paper. Section 2 presents a parametric investigation of antenna dimensions of the proposed work. In Sections 3 and 4, the results acquired by the simulation and measurement are discussed. The work's conclusion is presented in the final section.

2. PROPOSED WORK

2.1. Antenna Design

The proposed antenna features a rectangular patch made of Textile Shield IT material with dimensions 53.5 mm × 57.5 mm × 0.17 mm and a feed width of 6.67 mm as displayed in Figure 1. The patch is placed on a felt substrate with dimensions 67.33 mm × 63.22 mm × 1.5 mm and a dielectric constant of 1.2. The felt substrate is chosen for its compact and flexible textile material and is a high melt adhesive. The ground plane is made of copper with dimensions 67.33 mm × 63.22 mm × 0.035 mm. The antenna resonates at 2.4 GHz in the ISM band. The antenna design is simulated using CST software.

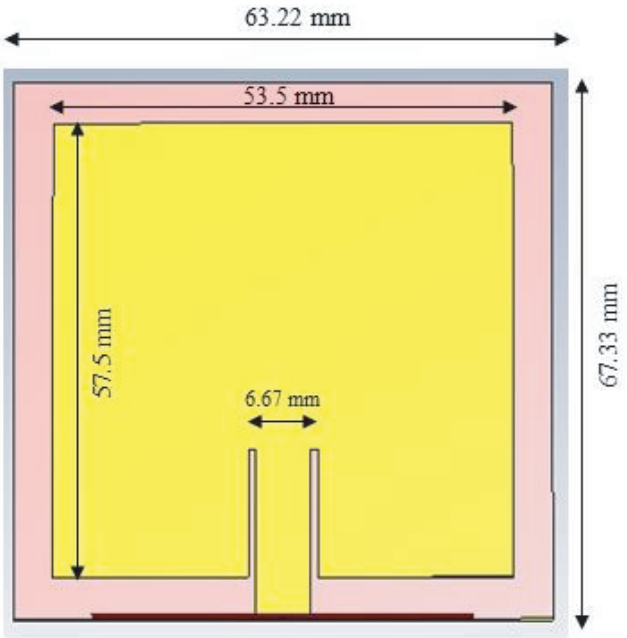

Figure 1. Textile-based rectangular patch antenna.

2.2. Metasurface Design

Metasurface antennas use metasurfaces to control and manipulate the behavior of electromagnetic waves, achieving a high degree of control over the radiation pattern and polarization of the emitted signal. While developing a metasurface, parameters like surface impedance and reflection coefficient are taken into account. The reflection coefficient of a metasurface depends on the geometry, properties, and arrangement of the resonant elements in the metasurface, as well as the polarization, angle, and frequency of the incident wave. It can be calculated from Equation (1)

$$\gamma = \frac{(Z_l - Z_s)}{Z_l + Z_s} \tag{1}$$

where z_l = characteristic impedance of the feed line.

The surface impedance Z_s can be illustrated as the electromagnetic properties of patches given by the Equation

$$Z_s = \frac{(R_s + jX_s)}{(w_0 * \varepsilon_0 * t)} \tag{2}$$

where R_s = surface resistance of the metasurface, X_s = surface reactance of the metasurface, w_0 = angular frequency of the operating frequency, ε_0 = permittivity of free space.

The radiation pattern of an antenna with the metasurface is derived from (3)

$$E_\theta = \frac{E_0 * \cos \emptyset * \cos \theta * \exp(-jkr)}{r} \tag{3}$$

where E_θ = magnitude of the electric field at the feed point, $\emptyset$ = azimuthal angle, θ = polar angle, k = wave number, r = distance from the feed point.

To improve the antenna's performance, metasurface unit cells made of textile Shield IT with dimensions of 24.6 mm × 24.6 mm × 0.17 mm are designed. The unit cells have an "I" shape with a length of 20 mm as displayed in Figure 2(a). The unit cells are arranged in a 2 × 2 and 3 × 3 array configuration as shown in Figures 2(b) and 2(c), and the antenna's performance is simulated. The results are shown in Table 1.

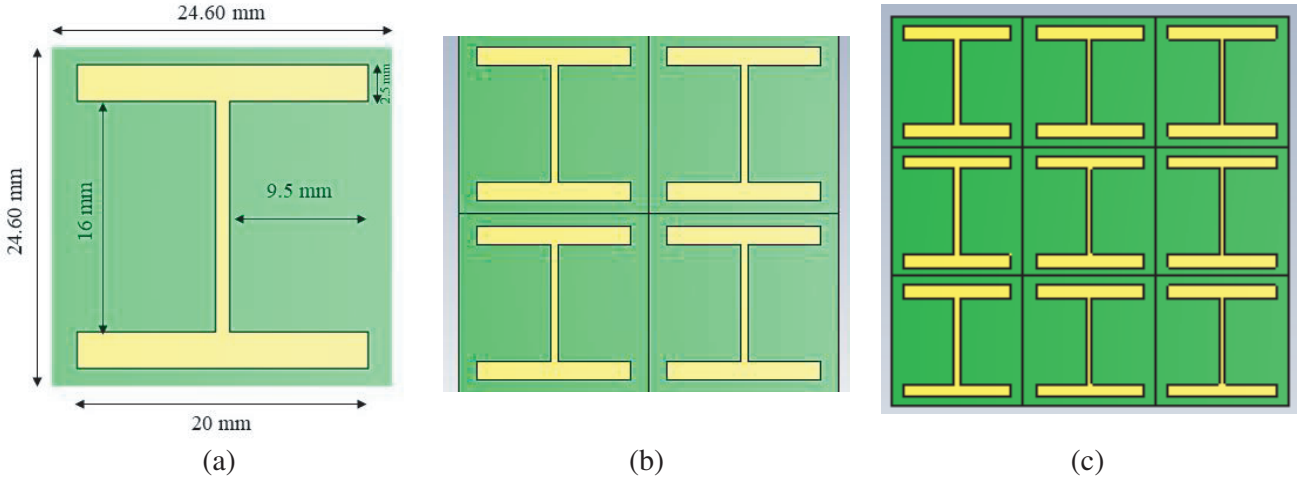

Figure 2. (a) MS unit cell with (b) 2 × 2 MS array, (c) 3 × 3 MS array.

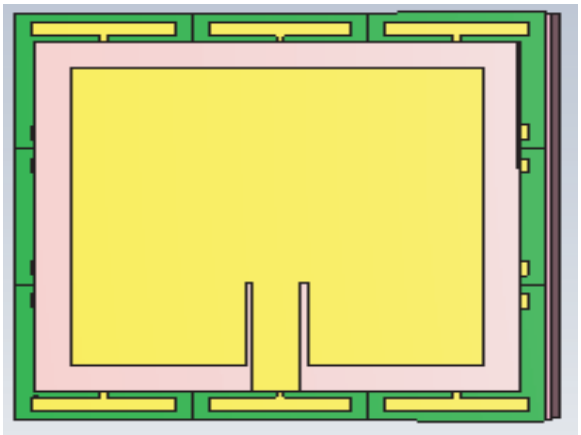

Figure 3. Textile-based rectangular patch antenna integrated with 3 × 3 metasurface.

Table 1. Simulation results of the antenna with metasurface.

Reflector type/ Radiation parameter	Return loss	Directivity (in dBi)	VSWR	Gain (in dBi)	Efficiency (in %)
Antenna with MS unit cell	−19.168	6.156	1.247	4.54	68.92
Antenna with 2 × 2 MS	−21.36	6.047	1.219	4.386	68.22
Antenna with 3 × 3 MS	−20.49	6.935	1.208	6.268	81.10

The designed antenna is integrated with the 3 × 3 metasurface consisting of I-shaped unit cells as depicted in Figure 3. The obtained results are displayed in Figure 4. It is inferred that the design obtains resonance at 2.4 GHz with a −20 dB, as displayed in Figure 4.

The simulation results in Table 1 show that the antenna with a 3×3 array metasurface configuration has the lowest return loss, highest directivity, gain, and efficiency.

2.3. Electromagnetic Band Gap Structure

EBG-based wearable antennas are similar to metasurface-based antennas in that they use an electromagnetic bandgap structure to enhance antenna performance. However, EBG structures typically consist of periodic metal or dielectric structures, while metasurfaces use sub-wavelength periodic structures to manipulate the phase and amplitude of incident electromagnetic waves. One advantage of EBG-based antennas is that they can provide improved isolation between antennas on a wearable

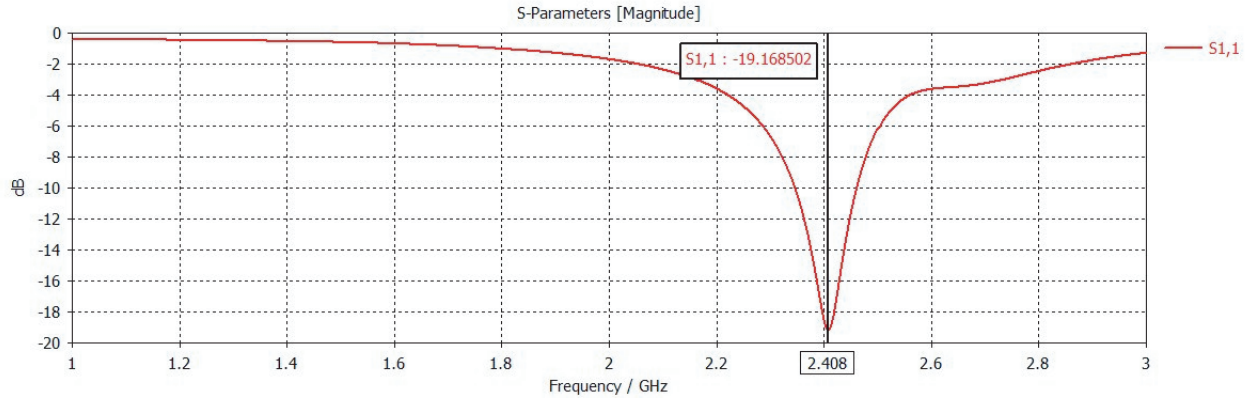

(a)

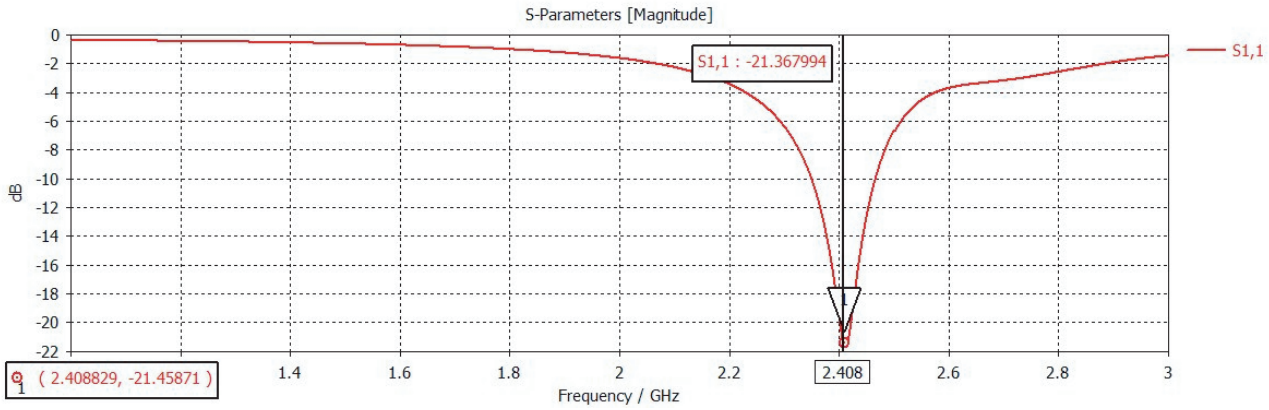

(b)

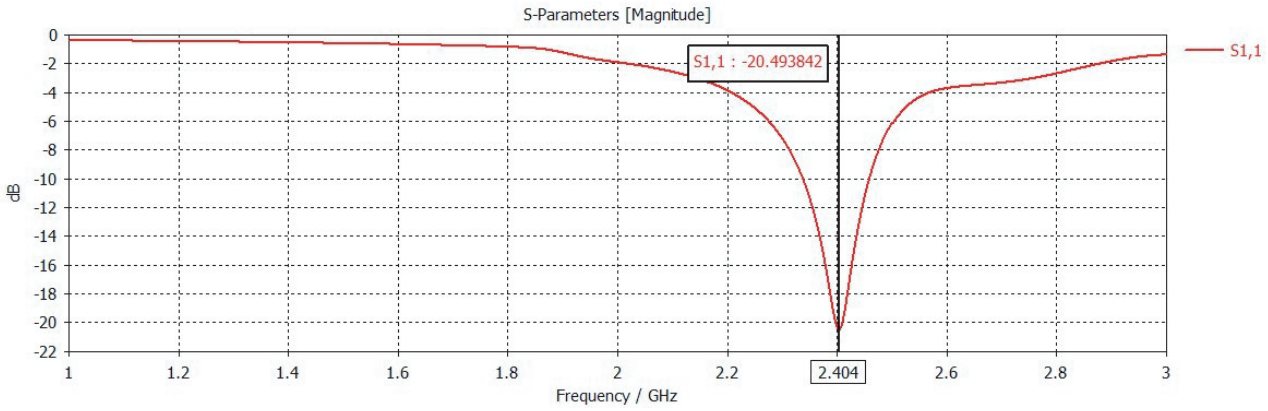

(c)

Figure 4. Reflection coefficient (S_{11}) of antenna with (a) metasurface unit cell, (b) 2×2 metasurface array, (c) 3×3 metasurface array.

device [16]. This is because the EBG structure can suppress surface waves that can lead to crosstalk between antennas. In contrast, metasurface-based antennas may not provide as much isolation between antennas.

The structure of EBG displays a photonic bandgap, which is a range of frequencies or wavelengths for which the propagation of electromagnetic waves is forbidden. This is due to the periodic nature of the EBG structure. The bandgap frequency of the EBG structure can be derived from Equation (4)

$$f_{bg} = \frac{c}{2} * \sqrt{\varepsilon}_{eff} * \sqrt{1 + \left(\frac{2\pi}{d}\right)^2} \tag{4}$$

where d is the spacing between the EBG unit cells. When an incident wave with a frequency within the bandgap is incident on the EBG structure, it is reflected with a phase shift determined by the equation below.

$$\varphi_r = -2\pi * f_{bg} * \frac{d}{c} \tag{5}$$

Figure 5 shows a typical EBG structure consists of a grounded dielectric substrate with a metallic patch positioned on top. The patch is designed in the shape of a mushroom consisting of a stem and a cap. The stem functions as a short circuit, whereas the cap functions as an open circuit. The capacitance

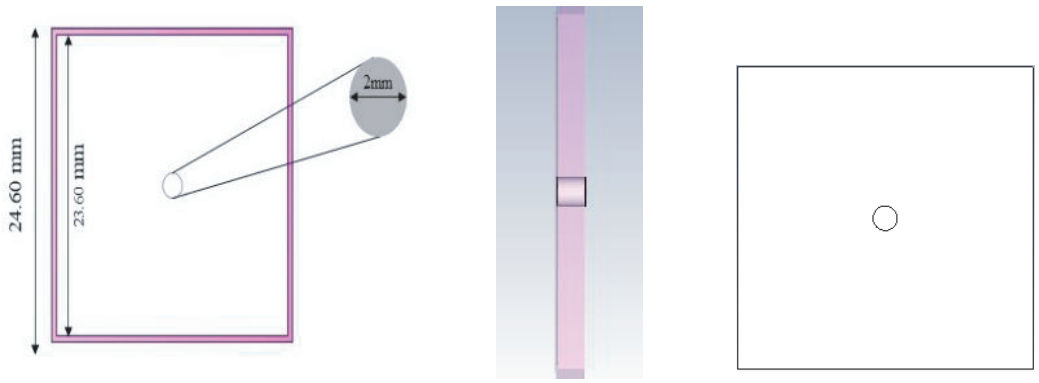

(a) (b) (c)

Figure 5. EBG unit cell. (a) Front view. (b) Side view. (c) Back view.

and inductance values for EBG unit cell are calculated from (6)

$$C = \frac{\varepsilon_0 + A}{d}$$
$$L = \frac{\mu_0 + h}{A} \tag{6}$$

where μ_0 and ε_0 are the permeability and permittivity of free space; A is the area of the EBG unit cell; h is the height of the substrate; and d is the spacing between the EBG unit cells. Changes in the dielectric constant of an EBG antenna affect the relationship between its inductor and capacitor, altering the antenna's impedance properties.

To make the EBG unit cell more compact, the series capacitance was increased. As a result, the unit cell was altered from Equation (1) as derived in [16]. These components together generate a high-impedance surface, which is capable of reflecting and suppressing undesired radiation. The equations for the resonant frequencies of the EBG structure are f_1 and f_2 and are given by:

$$f_1 f_2 = \frac{1}{2\pi\sqrt{L_R\left(C_L + C\right)}},\ \frac{1}{2\pi\sqrt{L_L C_R}} \tag{7}$$

The EBG mushroom design comprises a cylindrical-shaped via and a square patch that exhibits varying transmission properties, which are influenced by factors including patch size, via diameter, unit element spacing, substrate thickness, and substrate material. The patch is made of copper that has a thickness of 0.035 mm and is mounted on a material made of felt of 1.002 mm thickness. The substrate used is felt which is compact and flexible. The unit elements measure 23.60 mm × 23.60 mm with a 1 mm gap between each other, and features a via diameter of 1 mm. A total of nine unit cells are arranged on the substrate. The unit cells of the EBG are arranged in a 2 × 2 and 3 × 3 array configurations as shown in Figure 6, and the plots for S-parameters are specified in Figure 9, respectively.

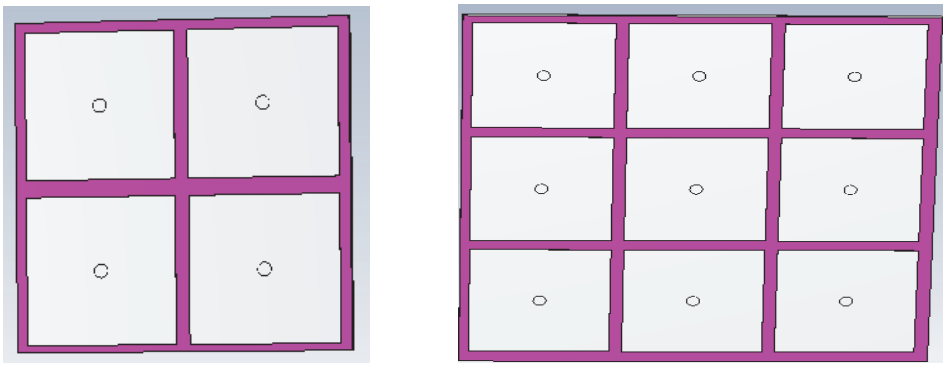

(a) (b)

Figure 6. Design of EBG unit cell with (a) 2 × 2 EBG, (b) 3 × 3 EBG.

Figure 6 shows the design of the EBG unit cell with 2 × 2 and 3 × 3 EBG configurations. Figure 7 shows a textile-based rectangular patch antenna integrated with a 3 × 3 EBG array. However, the integrated antenna with only an EBG structure results in increased return loss, which causes degradation in the antenna performance, as the acquired results seem inefficient [21]. To overcome this drawback, a new pattern of the antenna is designed, combining the antenna with both metasurface and EBG structures. This approach helps in arriving at the desired results of decreased return loss and SAR values with improved gain. The antenna structure combining metasurface with EBG is shown in Figure 8. Here, foam is positioned between the EBG and the antenna to absorb the excess heat radiated from the antenna.

The antenna integrated with the MS and EBG unit cell has a gain of 4.62 dBi, while the antenna with the 2 × 2 MS with EBG has a gain of 4.561 dBi. The antenna with 3 × 3 MS with EBG has the

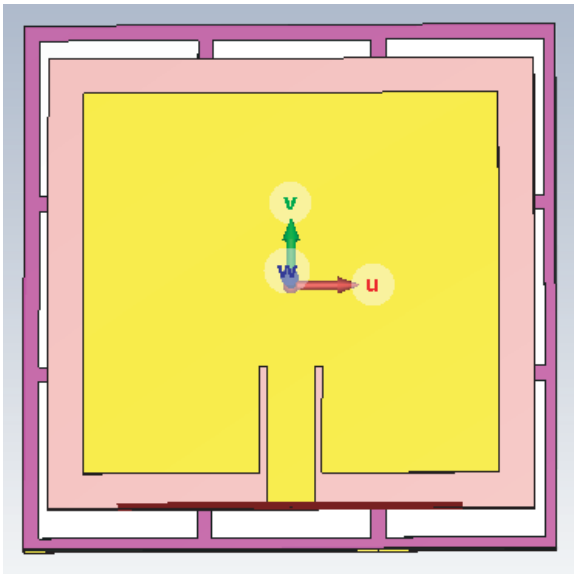

Figure 7. Textile-based rectangular patch antenna integrated with 3 × 3 EBG.

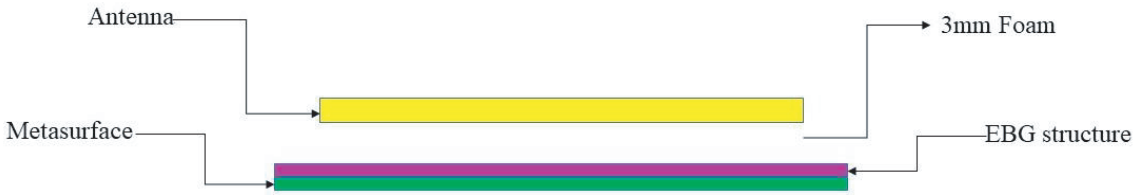

Figure 8. Textile-based rectangular patch antenna integrated with 3 × 3 metasurface and EBG structure.

highest gain of 6.375 dBi as shown in Figure 10(b). It can be inferred that the MS unit cell helps in increasing the gain of the antenna, leading to better signal strength.

One of the main advantages of EBG-based wearable antennas is that they can effectively reduce surface wave and backward radiation, which can improve the efficiency of the antenna as depicted in Table 2, and the antenna gain is also enhanced comparatively.

Table 2. Radiation parameters of the antenna with metasurface and EBG and MS.

Reflector type/ Radiation parameter	Return loss	Directivity (in dBi)	VSWR	Gain (in dBi)	Efficiency (in %)
Antenna with MS and EBG	−19.79	6.270	1.23	4.62	68.34
Antenna with 2 × 2 MS and EBG	−19.55	6.206	1.235	4.561	68.47
Antenna with 3 × 3 MS and EBG	−19.54	7.102	1.353	6.375	84.571

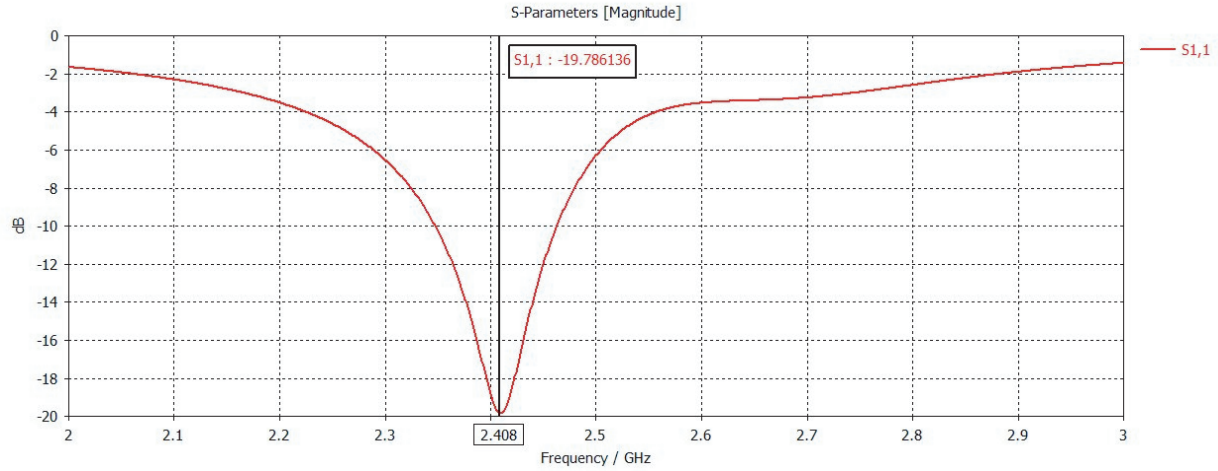

(a)

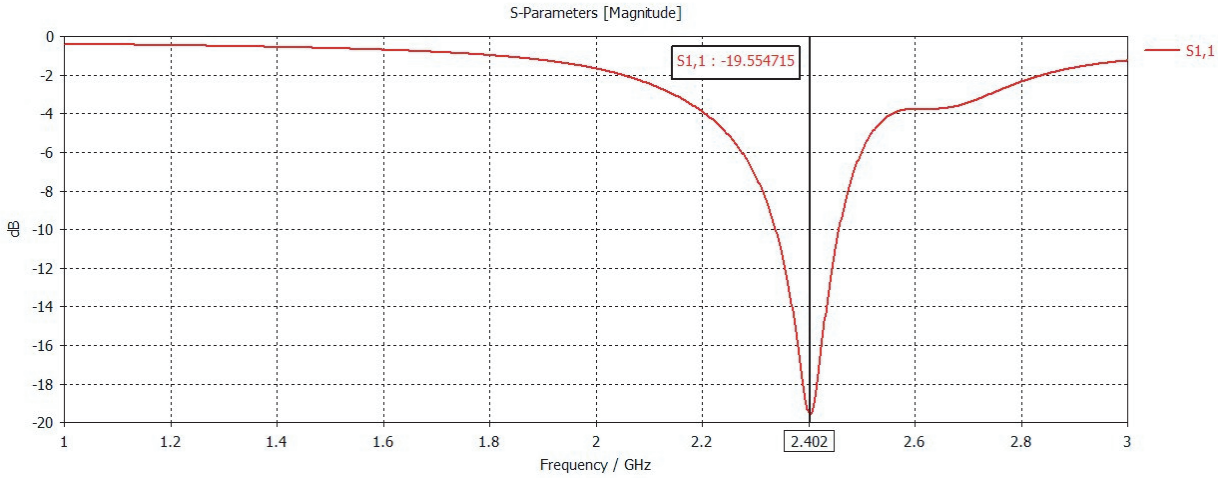

(b)

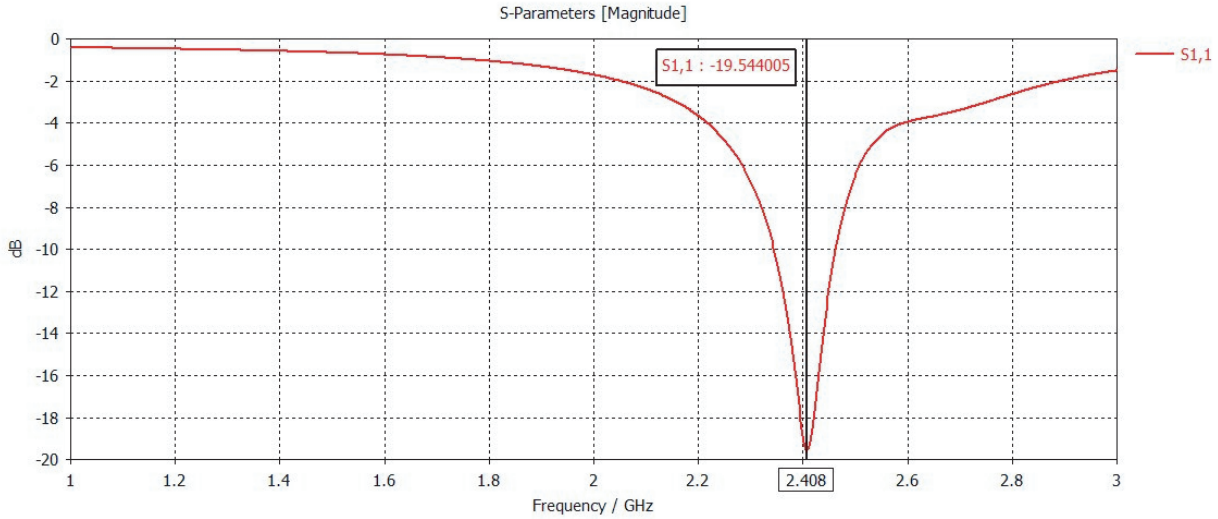

(c)

Figure 9. Reflection coefficient (S_{11}) of antenna with (a) EBG unit cell, (b) 2×2 EBG array, (c) 3×3 EBG array.

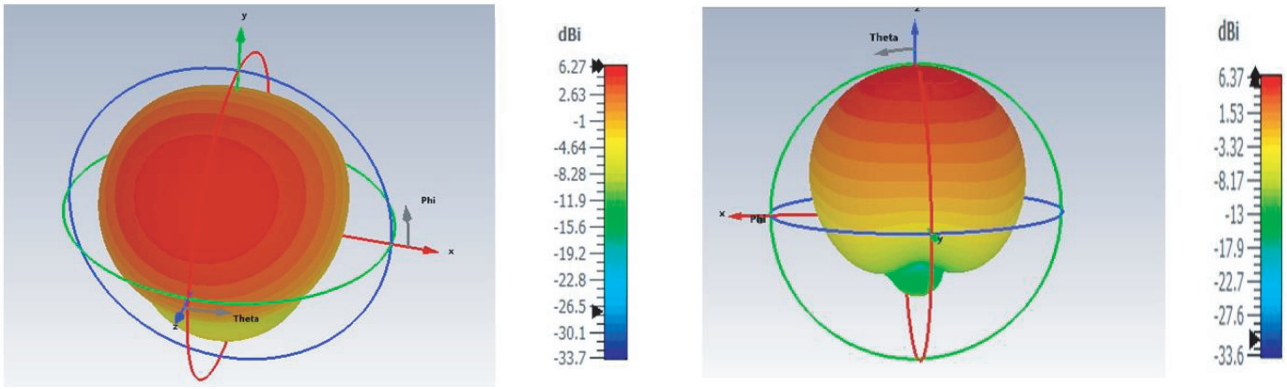

(a) (b)

Figure 10. Radiation pattern of the antenna integrated with (a) MS, (b) EBG and MS.

3. INTEGRATED ANTENNA CONFIGURATION OVER HUMAN MODEL

In this paper, a flat multilayer phantom model is designed in CST, and the integrated patch antenna is placed as shown in Figure 11. The goal of the integrated antenna is to make it applicable to wearable technology.

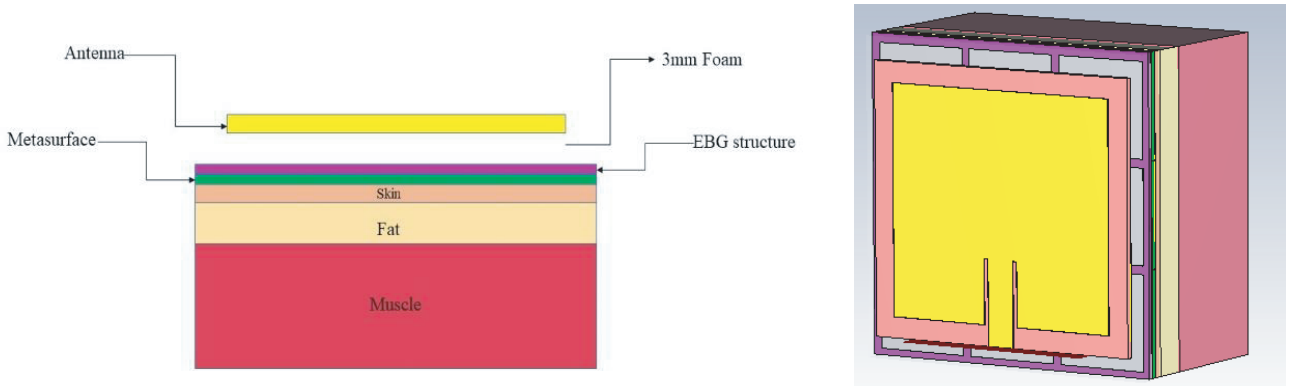

(a) (b)

Figure 11. (a) Lateral-view of the integrated antenna over the phantom model. (b) Antenna integrated over a three-layer phantom model.

As illustrated in Figure 11, a test setup has been arranged to measure its radiation on the human thigh for evaluating SAR. To mimic the human tissue model, a three-layered model is utilized to support the integrated antenna. This multi-layer model consists of fat, skin, and muscle [22]. A foam layer of 3 mm separates the presented antenna from the EBG structure. The SAR result must be considered to guarantee the antenna's compatibility with wearable applications. The thickness of the model is separated into 2 mm of skin, 30 mm of muscle, and 5–12.5 mm of fat. The electrical and thermal conductivity, density, metabolic rate of the human tissue layers are determined as listed in Table 3, taking into account that the dielectric properties of human tissue vary with frequency.

Table 3. Electromagnetic (EM) properties of the multilayer human tissue model.

Thigh Tissue/EM Properties	Dielectric Constant	Density (kg/m^3)	Electrical Conductivity (S/m)	Thermal Conductivity (W/K/m)	Blood Flow (W/km^3)	Metabolic Rate (W/m^3)
Skin	69.45	1100	0.507	0.21	9100	2000
Fat	6.07	900	0.507	0.16	1700	300
Muscle	65.97	1080	0.708	0.42	2700	500

4. SAR EVALUATION

The measurement of SAR is crucial when researching the effects of body exposure to RF radiation. SAR is used to determine the safety of exposure to radio frequency Electromagnetic Field (EMF), as high levels of exposure can potentially cause harm to the body. Equation (8) defines the SAR, which represents the amount of energy absorbed per unit of body tissue, expressed in watts per kilogram (W/kg).

$$SAR = \frac{\sigma E^2}{\rho} \text{ (W/kg)} \tag{8}$$

The SAR calculation takes into account the root-mean-square electric field induced in the tissue (E, measured in volts per meter), the tissue density (ρ, measured in kilograms per cubic meter), and the tissue electrical conductivity (σ, measured in siemens per meter). The SAR value determines the maximum allowable exposure to electromagnetic fields.

It is important to examine the value of SAR with MS and EBG to verify that the design adheres to safety regulations. According to the safety limit established by the Federal Communications Commission (FCC), the SAR value should be below 1.6 W/kg over 1 gram of human tissue. To evaluate the antenna's safety, we calculated the specific absorption rate (SAR) values for various fat thicknesses (5 mm to 12.5 mm) using the Finite-Difference Time-Domain (FDTD) method [23]. The results are displayed in Table 4 and Table 5. From the obtained results, it can be noticed that the value of SAR tends to be reduced when an EBG structure is placed along with the metasurface as displayed in Figure 12.

From comparisons in Tables 4 and 5, it is observed that the SAR values determined for different thicknesses of fat tissues of the thigh muscle are comparatively low for the antenna when connected

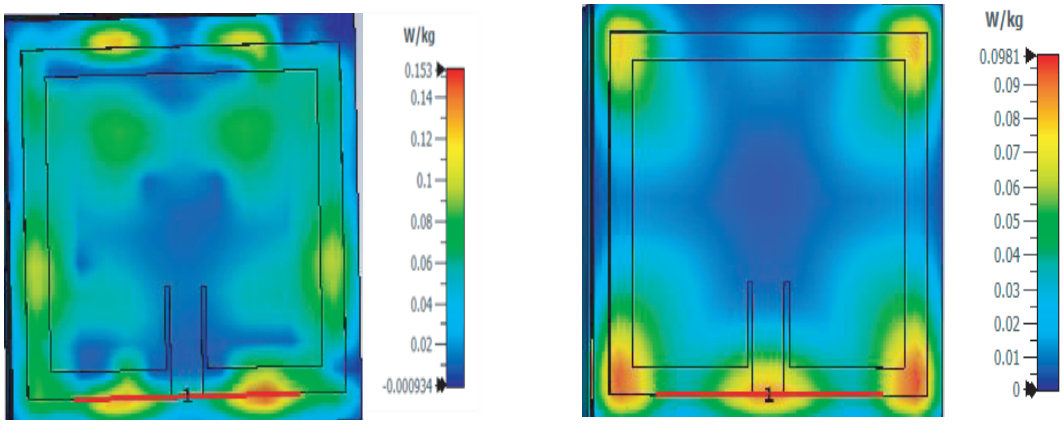

(a) (b)

Figure 12. Simulation of SAR levels over 10 mm of fat for (a) metasurface, (b) MS integrated with EBG.

Table 4. SAR results for the designed antenna with different metasurface configurations.

Reflector Type/Fat thickness	5 mm	6 mm	7.5 mm	8 mm	9 mm	10 mm	11 mm	12.5 mm
Antenna with MS unit cell	0.267	0.361	0.554	0.613	0.743	0.312	0.404	0.622
Antenna with 2×2 MS	0.348	0.364	1.053	1.219	1.306	0.829	0.441	1.24
Antenna with 3×3 MS	0.161	0.161	0.157	0.167	0.160	0.153	0.157	0.168

Table 5. SAR results for the designed antenna with different metasurface and EBG configurations.

Reflector Type/Fat thickness	5 mm	6 mm	7.5 mm	8 mm	9 mm	10 mm	11 mm	12.5 mm
Antenna with MS unit cell and EBG	0.247	0.283	0.312	0.288	0.308	0.359	0.383	0.371
Antenna with 2×2 MS and EBG	0.121	0.110	0.120	0.142	0.175	0.156	0.141	0.162
Antenna with 3×3 MS and EBG	0.0776	0.109	0.0907	0.0872	0.248	0.098	0.103	0.0939

Table 6. Comparison between the designed antenna and other related works.

References	Antenna physical size (mm^2)	Substrate type/ thickness (mm)	Reflector physical size (mm^2)/ type	Gain (dB)	Rad. Efficiency (%)	Max. SAR (W/kg) over 1 g of tissue
[8]	39×30	Rogers RO 3003/1.5	42×62/AMC	6.2	NA	0.66
[9]	30×25	Polyimide/0.05	74×74/ Metasurface	5.2	61.3	2.48
[12]	50×45	PDMS/3	24×40/ Metasurface	2.88	68.06	1.52
[14]	35×45	Felt/1.5	76×76/AMC	6.57	84.26	0.05
[17]	110×106	Viscose-wool felt/3	190×104/RIS EBG	5.8	NA	0.37
[24]	30×25	Felt/2	81×81/EBG	3.5	55	0.55
Proposed work	63×67	Felt/1.5	76×76/ Metasurface with EBG	6.37	82.4	0.077

structures of EBG and MS are synthesized than integration of the textile-based antenna with only metasurface [24]. The extensive comparison of antenna parameters is shown in Table 6.

On comparing these results, it can be observed that the use of the MS unit cell along with EBG in the textile-based patch antenna has led to significant improvements in the performance of the antenna in terms of efficiency, gain, directivity, and voltage standing wave ratio (VSWR). Furthermore, the specific absorption rate decreases by about 0.077 W/kg for 1 g of thigh tissue. However, further research is required to investigate the effects of the MS unit cell on other parameters such as bandwidth, radiation efficiency, and polarization.

5. CONCLUSION

This paper demonstrates that the design of a textile-based microstrip patch antenna is suitable for WBAN applications. The integration of metasurfaces with electromagnetic bandgap (EBG) beneath the antenna has proven to be highly effective in decreasing specific absorption rate (SAR) values and enhancing the efficiency and gain of the antenna in the ISM band frequency of 2.4 GHz. Furthermore, the effects of integrating metasurface and mushroom EBG structures for different thicknesses of fat have been investigated. It has been verified that the Specific Absorption Rate of the proposed antenna does not exceed the FCC limit of 1.6 W/kg at its operating frequency. As the substrate is lightweight, flexible, and soft, it makes the antenna easily wearable. Overall, the proposed work appears to advance the current state-of-the-art antenna design by leveraging the unique properties of metasurfaces to improve the performance of the antenna and minimize its impact on the human body. Overall, the innovative design of the textile-based microstrip patch antenna with a metasurface, EBG, and foam layer can be a promising solution for minimizing SAR in medical applications. The use of textile-based materials and the integration of metasurface and EBG allows for a comfortable and efficient transfer of energy, making it a suitable option for the use in medical applications.

REFERENCES

1. Ashya, A. Y. I., Z. Z. Abidin, S. H. Dahlan, H. Majid, S. M. Shah, M. R. Kamarudin, and A. Alomainy, "Compact and low-profile textile ebg-based antenna for wearable medical applications," *IEEE Antennas and Wireless Propagation Letters*, Vol. 16, 2550–2553, 2017.
2. Arnmanee, P., "Gain improvement of microstrip patch antenna using octagonal-loop metasurface superstrate and octagonal-shaped EBG structure for 2.4 GHz band application," *2018 15th International Conference on Electrical Engineering/Electronics, Computer, Telecommunications, and Information Technology*, 2018, 10.1109/ECTICon.2018.8619919.
3. Hariharan, V., S. Maheshwaran, S. Selvam, and N. Gunavathi, "Comparison of Electromagnetic Band Gap (EBG) structures for Specific Absorption Rate (SAR) reduction," *2015 Annual IEEE India Conference (INDICON)*, New Delhi, India, 2015.
4. Shaw, T. and D. Mitra, "Metasurface-based radiative near-field wireless power transfer system for implantable medical devices," *IET Microw. Antennas Propag.*, Vol. 13, No. 12, 1974–1982, Oct. 2019.
5. Kashani, M., L. Shafai, and D. Isleifson, "Performance improvement of a microstrip patch antenna on an EBG structure," *IEEE International Symposium on Antennas and Propagation and North American Radio Science Meeting*, Feb. 17, 2021.
6. Zaman, M. I., F. T. Hamedani, and H. Amjadi, "A New EBG structure and its application on microstrip patch antenna," *International Symposium on Antenna Technology and Applied Electromagnetics*, Aug. 9, 2012.
7. Alibakhshikenari, M., F. Babaeian, B. S. Virdee, S. Aïssa, L. Azpilicueta, C. H. See, A. A. Althuwayb, I. Huynen, F. Falcone, and E. Limiti, "A comprehensive survey on "Various decoupling mechanisms with focus on metamaterial and metasurface principles applicable to SAR and MIMO antenna systems," *IEEE Access*, Vol. 8, 192965–193004, Oct. 21, 2020.

8. Jiang, Z. H., D. E. Brocker, P. E. Sieber, and D. H. Werner, "A compact, low-profile metasurface-enabled antenna for wearable medical body-area network devices," *IEEE Transactions on Antenna and Propagation*, Vol. 62, No. 8, Aug. 2014.
9. Wang, M., Z. Yang, J. Wu, J. Bao, J. Liu, L. Cai, T. Dang, H. Zheng, and E. Li, "Investigation of SAR reduction using a flexible antenna with metamaterial structure in wireless body area network," *IEEE Trans. Antennas Propag.*, Vol. 66, No. 6, 3076–3086, Jun. 2018.
10. Zhang, K., G. A. E. Vandenbosch, and S. Yan, "A novel design approach for compact wearable antennas based on metasurfaces," *IEEE Trans. Biomed. Circuits Syst.*, Vol. 14, No. 4, 918–927, 2020.
11. Purohit, S. and F. Raval, "Wearable-textile patch antenna using jeans as substrate at 2.45 GHz," *International Journal of Engineering Research & Technology (IJERT)*, Vol. 3, No. 5, May 2015, ISSN: 2278-0181.
12. Janapala, D. K., M. Nesasudha, T. Mary Neebha, and R. Kumar, "Specific absorption rate reduction using metasurface unit cell for flexible polydimethylsiloxane antenna for 2.4 GHz wearable applications," *International Journal RF and Microwave Computer-aided Engineering*, 2019.
13. Sheeba, R. and T. Jayanthy, "Analysis and implementation of flexible microstrip antenna of soft substrates with different Feeding Techniques for ISM band," *Proceeding of International Conference on System, Computation, Automation, and Networking*, Oct. 24, 2019.
14. Youssef, O. M., M. El Atrash, and M. A. Abdalla, "A compact fully fabric I-shaped antenna supported with textile-based AMC for low SAR 2.45 GHz wearable applications," *Microwave Optical Technology Letters*, 2023.
15. Iqbal, K. and Q. U. Kha, "Review of metasurfaces through unit cell design an numerical extraction of parameters and their applications in antennas," *IEEE Access*, Vol. 10, 112368–11239, Oct. 13, 2022.
16. Azarbar, A. and J. Ghalibafan, "A compact low-permittivity dual-layer EBG structure for mutual coupling reduction," *International Journal of Antennas and Propagation*, Vol. 2011, Article ID 237454, 2011, doi: 10.1155/2011/237454.
17. Agus, A. N. S. S., T. Sabapathy, M. Jusoh, M. A. Abdelghany, K. Hossain, S. Padmanathan, S. S. Al-Bawri, and P. J. Soh, "Combined RIS and EBG surfaces inspired meta-wearable textile MIMO antenna using viscose-wool felt," *MDPI Journals*, 2022, doi: org/10.3390/polym14101989.
18. Althuwayb, A., M. Alibakhshikenari, B. S. Virde, N. Rashid, K. Kaaniche, A. B. Atitallah, A. Armghan, O. I. Elhamrawy, C. H. See, and F. Falcone, "Metasurface inspired flexible wearable MIMO array for wireless body area network applications and biomedical telemetry devices," *IEEE Access*, Vol. 11, Jan. 5, 2023.
19. Kumar, A., D. Ary, and D. K. Srivastava, "Band width of microstrip antenna improved by using mushroom type EBG structure," *IMPACT 2013*, IEEE, May 22, 2014.
20. Gnanagurunathan, G. and U. G. Udofia, "Performance analysis of the mushroom-like-EBG structure integrated with a microstrip patch antenna," *IEEE Asia-Pacific Conference on Applied Electromagnetics (APACE)*, Feb. 24, 2011.
21. Usman, F. and R. S. Yadav, "Wideband reconfigurable antenna for industrial, scientific and medical applications," *International Journal of Information Technology and Electrical Engineering (ITEE)*, Vol. 11, No. 2, Apr. 2022.
22. Sugunavathy, S., V. K. Sudha, and D. Parthiban, "Fabric woven textile antenna for medical applications," *Journal of Physics*, 012022–012022, 2021.
23. Akram, G. and Y. Jasmy, "Specific Absorption Rate (SAR) on the human head as function of orientation of plane wave radiation: FDTD-based analysis," *Second Asia International Conference on Modelling and Simulation (AMS)*, IEEE, May 23, 2008.
24. Gao, G.-P., B. Hu, S.-F. Wang, and C. Yang, "Wearable circular ring slot antenna with EBG structure for wireless body area network," *IEEE Antennas and Wireless Propagation Letters*, Vol. 17, No. 3, 434–437, 2018.
25. Balaji Vignesh, L. K. and K. Kavitha, "A Survey on fractal antenna design," *International Journal of Pure and Applied Mathematics*, Vol. 120, No. 6, 10941–10959, 2018.